Subcell I-V characteristic analysis of GaInP/GaInAs/Ge solar cells using electroluminescence measurements

Sebastian Roensch, Raymond Hoheisel,[a] Frank Dimroth, and Andreas W. Bett
Fraunhofer Institute for Solar Energy Systems, Heidenhofstraße 2, 79110 Freiburg, Germany

(Received 4 October 2010; accepted 30 May 2011; published online 23 June 2011)

The I-V characteristics of the individual subcells of a monolithic $Ga_{0.50}In_{0.50}P/Ga_{0.99}In_{0.01}As/Ge$ triple-junction solar cell have been extracted from measurements of the electroluminescence peak intensity as a function of the electroluminescence injection current. By using the spectral reciprocity relation between the electroluminescence and the quantum efficiency, the individual subcell I-V characteristics were derived. It is shown that the subcell dark I-V characteristics and the subcell illuminated I-V characteristics are accessible under variable spectral illumination conditions. © *2011 American Institute of Physics*. [doi:10.1063/1.3601472]

Multijunction solar cells have the potential to achieve much higher conversion efficiencies than single-junction devices due to an optimized utilization of the solar spectrum.[1] To realize multijunction solar cells, many material systems are under investigation; among them are III–V compound semiconductors,[2,3] organic materials,[4,5] chalcopyrites,[6,7] and silicon.[8,9] The performance of multijunction solar cells is strongly related to the individual current-voltage (I-V) characteristics of the respective subcells. Therefore, access to the individual subcell I-V characteristics is of essential importance for further optimization of multijunction solar cell structures and devices. However, most multijunction solar cell technologies are based on a monolithic structure. As a consequence, the subcells do not have individual contact pads, and the I-V characteristics cannot be directly measured.

A possible method to obtain detailed information about the desired subcell performance is the optoelectronic reciprocity relation between the spectrally resolved electroluminescence (EL) and the external quantum efficiency (EQE)[10] provided that the subcells have sufficient high mobility.[11] The validity of the optoelectronic reciprocity relation has been demonstrated in an III–V lattice-mismatched $Ga_{0.35}In_{0.65}P/Ga_{0.83}In_{0.17}As/Ge$ solar cell.[12] This type of III–V triple-junction (3J) solar cell is designed so that all three subcells generate the same photocurrent under standard testing conditions.[13] In real world applications, however, the solar spectrum varies over the course of the day, and as a result the 3J cell operates under current-mismatched conditions, i.e., each subcell generates different current densities. In this contribution we show that the application of the reciprocity relation allows an accurate subcell characterization even under significant current-mismatched conditions. The measurements were conducted with lattice-matched $Ga_{0.50}In_{0.50}P/Ga_{0.99}In_{0.01}As/Ge$ solar cells,[14,15] whose subcells evidence a high degree of current-mismatch under terrestrial and extraterrestrial standard illumination conditions. This type of 3J solar cell achieves the highest conversion efficiency among today's solar cell technologies.[16] Figure 1 shows the spectrally resolved EL and EQE of a 2×2 cm^2 3J solar cell. All measurements were carried out at a constant ambient temperature of 298 K. The EL measurements were realized with a double monochromator and lock-in technique. The EL signal of the $Ga_{0.50}In_{0.50}P$-top and $Ga_{0.99}In_{0.01}As$-middle subcell was investigated with a calibrated Si detector. An additional calibrated GaInAs detector was used for the measurement of the EL signal of the Ge-bottom subcell. The EQE measurements were performed according to Meusel *et al.*[17] Subsequently, the EL peak intensity of the three subcells was measured at different EL injection current-densities between 0.5 and 530 mA/cm^2, see Fig. 2. The sensitivity of the detector limits the measurement in the low EL injection current range. Therefore, a linear extrapolation is used in this range for further analysis.

The derivation of the I-V characteristics follows the approach used by Kirchartz *et al.*[12] and additionally includes

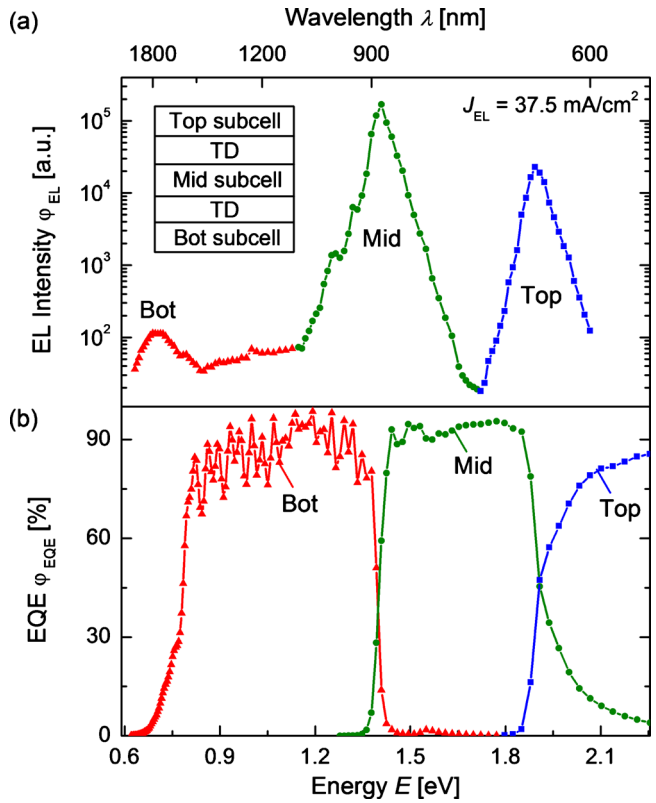

FIG. 1. (Color online) (a) Spectrally resolved EL spectrum and (b) EQE of a 3J solar cell (insert) built up by a $Ga_{0.50}In_{0.50}P$ top (top), a $Ga_{0.99}In_{0.01}As$ middle (mid) and a Ge bottom (bot) subcell monolithically connected via tunneling diodes (TD).

[a]Electronic mail: raymond.hoheisel@ise.fraunhofer.de.

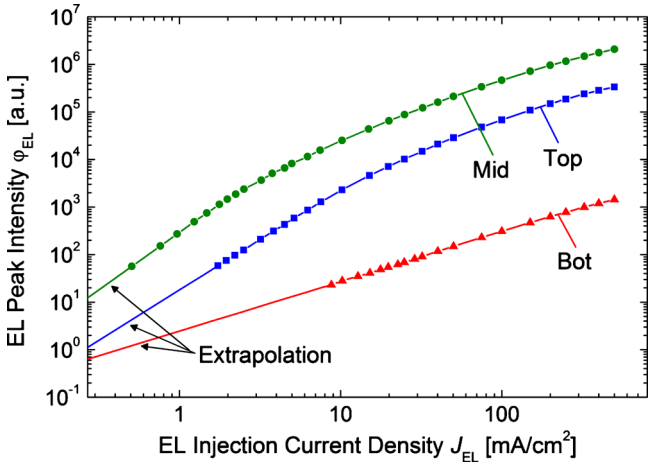

FIG. 2. (Color online) EL peak intensity φ_{EL} of the top, middle, and bottom subcells vs EL injection current density J_{EL}.

the individual photocurrent density of the subcells. The spectral reciprocity relation is given by[10,12]

$$\varphi_{EL,i}(J_{EL}) = \varphi_{EQE,i} \cdot \varphi_{BB}\left[\exp\left(\frac{qV_i(J_{EL})}{kT}\right) - 1\right], \quad (1)$$

where $\varphi_{EL,i}$ is the intensity of the EL peak signal depending on the EL injection current density J_{EL}, $\varphi_{EQE,i}$ and φ_{BB} describe the EQE and the black body photon flux with respect to the photon energy E of the EL peak of the subcell i, q is the elementary charge, V_i is the current density dependent voltage of the subcell i, k is the Boltzmann constant, and T is the absolute temperature. Using the Boltzmann approximation, [Eq. (1)] can be reformulated to[12]

$$V_i(J_{EL}) = \frac{kT}{q}\ln[\phi_{EL,i}(J_{EL})] + \frac{E}{q} - 2\frac{kT}{q}\ln(E) - \frac{kT}{q}\ln(\varphi_{EQE,i}) - \frac{kT}{q}\ln(C) = V_i^*(J_{EL}) - \delta V \quad (2)$$

[Equation (2)] allows the determination of the voltage of each subcell V_i, except for the voltage offset $\delta V = kT/q \cdot \ln(C)$ with C being a constant factor.[12] The voltage offset δV, which is constant for all individual subcells, can be determined by considering the subcells are monolithically connected in series. Assuming the 3J solar cell operates under open-circuit conditions, the voltage of the 3J device is given with [Eq. (2)] by

$$V_{OC,3J} = V_{OC,top} + V_{OC,mid} + V_{OC,bot} = V_{OC,top}^* + V_{OC,mid}^* + V_{OC,bot}^* - 3 \cdot \delta V. \quad (3)$$

Since the open circuit voltage depends on the spectral intensity of the illumination, it is also linked to the photocurrent density under the applied spectrum $\varphi_{spec}(\lambda)$. The photocurrent density $J_{Photo,i}$ was calculated from the EQE $\varphi_{EQE,i}(\lambda)$ by

$$J_{Photo,i} = \frac{q\lambda}{hc}\int \varphi_{EQE,i}(\lambda) \cdot \varphi_{spec}(\lambda)d\lambda, \quad (4)$$

where λ is the wavelength, h is the Planck constant, and c is the speed of light. The voltage offset δV was subsequently determined by rearranging [Eq. (3)] to

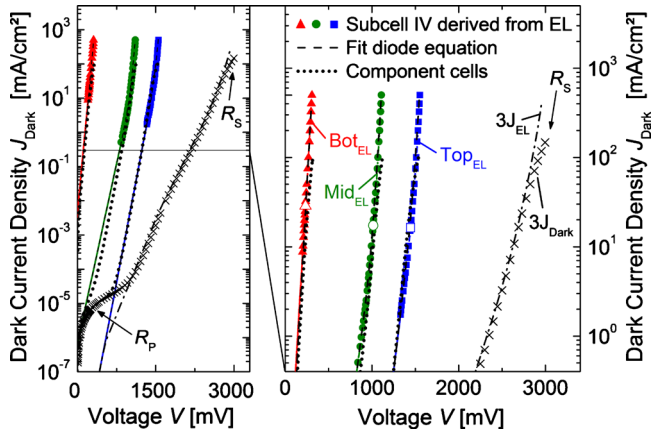

FIG. 3. (Color online) I-V characteristics of the top, middle, and bottom subcells and of the 3J solar cell derived from EL and EQE measurements. The open symbols of the subcell I-V curves mark the points used for calibration. The plot includes also the directly measured dark I-V curve of component cells and of the 3J solar cell containing series resistance R_S and parallel resistance R_P.

$$\delta V = \frac{1}{3}\left[\sum_{i=1}^{3} V_i^*(J_{EL,i} = J_{Photo,i}) - V_{OC,3J}\right]. \quad (5)$$

[Equation (5)] requires the voltage values V_i^* for $J_{EL,i} = J_{Photo,i}$ because only in this case the internal subcell voltages during the EL measurement correspond to those under open-circuit conditions. This approach is an improvement on the method of Kirchartz *et al.*[12] in that it applies to a current-mismatched situation as the generated internal photocurrent in each subcell at V_{OC} is calculated from the measured EQE and known spectrum. The points used for the calibration are marked by open symbols in Fig. 3. These current values correspond to the photocurrent densities under the AM0 reference spectrum[18] and the sum of these voltages is equal by design to the open circuit voltage under AM0. Subsequently, the same voltage offset δV was applied on all other subcell I-V points for calibration because δV and therefore also C are independent of the EL injection current density J_{EL}, see [Eq. (2)]. Thus, the calibration with δV could in principle also be performed at other sun simulator concentration levels.

The resulting calibrated dark I-V curves ($J_{Dark,i} = J_{EL,i}$) of the top, middle, and bottom subcell are shown in Fig. 3. The results in the low current range, depicted by the continuous lines, are derived from the extrapolation of the measured EL peak intensity shown in Fig. 2. The slope of the I-V curve changes for the top and the middle subcell indicating different diode quality factors. The values of the diode quality factors n were determined by fitting the derived curves to the 2-diode equation. The diode quality factor in the high bias range was set $n_1 = 1$, whereas the diode quality factor in the low bias range n_2 was derived from the fit. The resulting values are $n_{2,top} = 2.18$ for the top cell and $n_{2,mid} = 2.48$ for the middle subcell which indicates that the low bias range is dominated by Shockley-Read-Hall (SRH) recombination. The curve of the bottom subcell was fitted to the 1-diode equation ($n = 1$), since the slope does not significantly change. The fitted curves match the EL curves over the entire voltage range verifying the assumption of $n_1 = 1$ and the derived n_2 values for the top and middle subcell.

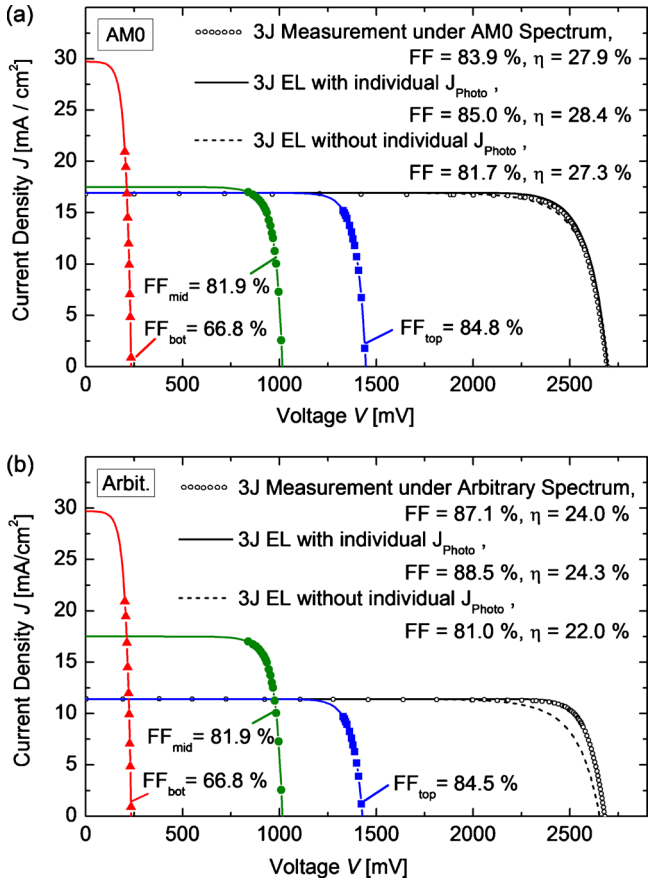

FIG. 4. (Color online) I-V characteristics with FF and efficiency (η) of a 3J solar cell and its subcells under (a) the AM0 reference spectrum and (b) an arbitrary spectrum. Both plots include the directly measured I-V curve of the 3J solar cell containing resistive effects. For comparison, the plot shows also the results obtained without consideration of the individual photo current density.

In addition, the derived subcell EL I-V curves were compared to corresponding component (isotype) cells, see Fig. 3. These curves also verify the subcell I-V-characteristics obtained from the EL measurements. The n_2 values of the component cells ($n_{2,\mathrm{top}}$=2.11 and $n_{2,\mathrm{mid}}$=2.17) confirm that the low bias range is dominated by SRH recombination.

For further verification, the directly measured dark I-V curve of the 3J device (Fig. 3: $3J_{\mathrm{Dark}}$) was compared with the sum of the derived subcell I-V curves (Fig. 3: $3J_{\mathrm{EL}}$). Although the derived subcell I-V curves were calibrated only with a single set of I-V points the sum of the subcell voltages reproduces the directly measured dark I-V curve of the 3J device up to the range dominated by the series and parallel resistance.

To give confidence in the validity of the method presented above and to demonstrate its utility in a strongly current-mismatched situation, we have measured the light I-V curve of the 3J cell (Fig. 4(a) open circles) under two different spectra and compared then with the predictions obtained from the summation of the subcell dark characteristics (Fig. 4: 3J EL with individual J_{Photo}). The two spectra chosen were the AM0 reference spectrum also used for the calibration of the derived voltage values and an arbitrary, but known, spectrum with reduced intensity in the blue so that the top subcell severely limited the 3J current. The subcell I-V curves were derived according to the principle of superposition by subtracting the corresponding photocurrent density leading to $J_{\mathrm{SC},i}=J_{\mathrm{Photo},i}$. In both cases, AM0 and the applied arbitrary spectral condition, an excellent agreement within the measurement uncertainty of 2% can be observed between the 3J I-V curve derived from EL and the 3J I-V curve directly measured, verifying the applicability of the described method. For comparison, the I-V characteristics were also derived for the same 3J device by applying the method for current-matched devices according to Kirchartz *et al.*[12] For this purpose $V_i^*(J_{\mathrm{EL},i}=J_{\mathrm{Photo},i})$ in [Eq. (5)] was replaced by $V_i^*(J_{\mathrm{EL},i}=J_{\mathrm{SC,3J}})$ and all three resulting dark I-V curves were adjusted to the short circuit current density of the 3J device (Fig. 4: 3J EL without individual J_{Photo}). Figure 4 also includes the fill factor (FF) and efficiency (η). The parameters derived from the measured 3J I-V curve are slightly reduced compared to the parameters determined from the EL measurement because of the present series resistance R_{S} and the parallel resistance R_{P} in the I-V measurement. Neglecting resistive effects, the method can be used, in principle, to estimate the performance of the 3J device under any spectrum of interest without the need of an experimentally realized spectrum for each operating scenario.

In summary, the presented subcell I-V characteristics of $Ga_{0.50}In_{0.50}P/Ga_{0.99}In_{0.01}As/Ge$ solar cells verify the application of the reciprocity relation to multijunction solar cells whose subcells evidence a high current mismatch. The results also demonstrate that the same set of EL measurements can be employed to derive the I-V curves of the subcells in the dark and under variable spectral illumination conditions.

[1]C. H. Henry, J. Appl. Phys. **51**, 4494 (1980).
[2]J. F. Geisz, D. J. Friedman, J. S. Ward, A. Duda, W. J. Olavarria, T. E. Moriarty, J. T. Kiehl, M. J. Romero, A. G. Norman, and K. M. Jones, Appl. Phys. Lett. **93**, 123505 (2008).
[3]M. Yamaguchi, K.-I. Nishimura, T. Sasaki, H. Suzuki, K. Arafune, N. Kojima, Y. Ohsita, Y. Okada, A. Yamamoto, T. Takamoto, and K. Araki, Sol. Energy **82**, 173 (2008).
[4]A. G. F. Janssen, T. Riedl, S. Hamwi, H.-H. Johannes, and W. Kowalski, Appl. Phys. Lett. **91**, 073519 (2007).
[5]X. W. Sun, D. W. Zhao, L. Ke, A. K. K. Kyaw, G. Q. Lo, and D. L. Kwong, Appl. Phys. Lett. **97**, 053303 (2010).
[6]M. Schmid, J. Krč, R. Klenk, M. Topič, and M. Ch. Lux-Steiner, Appl. Phys. Lett. **94**, 053507 (2009).
[7]M. van Schilfgaarde, T. J. Coutts, N. Newman, and T. Peshek, Appl. Phys. Lett. **96**, 143503 (2010).
[8]M. N. van den Donker, A. Gordijn, H. Stiebig, F. Finger, B. Rech, B. Stannowski, R. Bartl, E. A. G. Hamers, R. Schlatmann, and G. J. Jongerden, Sol. Energy Mater. Sol. Cells **91**, 572 (2007).
[9]T. Söderström, F. J. Haug, X. Niquille, V. Terrazoni, and C. Ballif, Appl. Phys. Lett. **94**, 063501 (2009).
[10]U. Rau, Phys. Rev. B **76**, 085303 (2007).
[11]T. Kirchartz and U. Rau, Phys. Status Solidi A **205**, 2737 (2008).
[12]T. Kirchartz, U. Rau, M. Hermle, A. W. Bett, A. Helbig, and J. H. Werner, Appl. Phys. Lett. **92**, 123502 (2008).
[13]W. Guter, J. Schöne, S. P. Philipps, M. Steiner, G. Siefer, A. Wekkeli, E. Welser, E. Oliva, A. W. Bett, and F. Dimroth, Appl. Phys. Lett. **94**, 223504 (2009).
[14]R. R. King, D. C. Law, K. M. Edmondson, C. M. Fetzer, G. S. Kinsey, H. Yoon, R. A. Sherif, and N. H. Karam, Appl. Phys. Lett. **90**, 183516 (2007).
[15]F. Dimroth, Phys. Status Solidi C **3**, 373 (2006).
[16]M. A. Green, K. Emery, Y. Hishikawa, and W. Warta, Prog. Photovoltaics **18**, 346 (2010).
[17]M. Meusel, C. Baur, G. Siefer, F. Dimroth, A. W. Bett, and W. Warta, Sol. Energy Mater. Sol. Cells **90**, 3268 (2006).
[18]ISO 15387, International Organization for Standardization, 2005.